



HAL
open science

Internal Ceramic Protective Coating of Hollow-Core Fibers

Jenny Jouin, Philippe Thomas, Heloïse Orihuel, Elodie de Sousa, Yann Launay, Lyna Torzuoli, Benoit Debord, Ali Al-dhaybi, Frédéric Gérôme, Fetah Benabid

► **To cite this version:**

Jenny Jouin, Philippe Thomas, Heloïse Orihuel, Elodie de Sousa, Yann Launay, et al.. Internal Ceramic Protective Coating of Hollow-Core Fibers. *Advanced Engineering Materials*, 2024, pp.20302209. 10.1002/adem.202302209 . hal-04574276

HAL Id: hal-04574276

<https://hal.science/hal-04574276>

Submitted on 14 May 2024

HAL is a multi-disciplinary open access archive for the deposit and dissemination of scientific research documents, whether they are published or not. The documents may come from teaching and research institutions in France or abroad, or from public or private research centers.

L'archive ouverte pluridisciplinaire **HAL**, est destinée au dépôt et à la diffusion de documents scientifiques de niveau recherche, publiés ou non, émanant des établissements d'enseignement et de recherche français ou étrangers, des laboratoires publics ou privés.

Internal Ceramic Protective Coating of Hollow-Core Fibers

Jenny Jouin,* Philippe Thomas, Heloïse Orihuel, Elodie De Sousa, Yann Launay, Lyna Torzuoli, Benoit Debord, Ali Al-Dhaybi, Frédéric Gérôme, and Fetah Benabid

Dedicated to Nahum Travitzky

To optimize the use of hollow-core photonic crystal fibers (HC-PCF), their cores are filled with an atomic gas for an ultra-enhanced interaction with an incident laser beam in applications such as atomic vapor microcells. One challenge in these gas-filled HC-PCFs is to control the physiochemical interactions between the gas medium and the silica inner surface of the fiber core surround. In this work, thus, the processing of ceramic coatings on glass substrates by chemical solution deposition is focused on. Also, the successful implementation of an original coating procedure for a deposition inside hollow-core fibers with complex microstructures is described. It is indeed possible to form a thin, dense, inorganic, and amorphous layer with a low thickness, low roughness, and high transparency. To obtain such a result, several parameters must be controlled, including the concentration of the solution, the technique and the deposition time, as well as the heat treatment undergone by the fiber. In particular, the selected aluminosilicate coatings, which are nonporous and present a 20–30 nm thickness, demonstrate a considerable improvement of the lifetime properties of the fibers filled with rubidium vapor, without modifying its original guiding properties.

down from high values superior to the dB m^{-1} level to 0.174 dB km^{-1} in the telecom range,^[1,4] with a transmission window opened from the UV to IR ranges.^[5–7] This improvement of the performances and range of use in the HC-PCF is strongly related to the complexification of the design of their inner structures. As an example, we can cite the generalization of negative curvature-based shapes, associated with small angles used to create point defects as far as possible from the central guiding area delimited by the silica cladding,^[8–10] or the recent work on the rugosity of the inner core of the fiber, decreasing its losses in the UV/visible spectral range: $(0.9–50 \text{ dB km}^{-1})$.^[11] These properties lead to their use as atomic vapor microcells, by filling their core with an atomic gas such as Rb or Cs for example. This gas can then interact with the guided light and enhance its properties.^[12–14]

One limitation that can arise in these systems is the temporal stability of the performances, related with the longevity of the gas, or the fragility of the devices. This kind of phenomena occurs in metrology applications, as the atomic gas, which is inserted inside the fiber to interact with the transported light, can be deteriorated by two main phenomena. The first one is its loss by being adsorbed at the silica surface,^[15] and the second one being its degradation in quality following the outgassing of the fiber inside its own core.^[16] Also, in the case of power offset applications, the inner core can be irreversibly thermally damaged, which limits the use of the fibers.^[17] In these particular cases, a functionalization of the inner core of the structure can be considered. For this, a protective coating can be applied at the inner gas/silica interface, its main properties being to be dense enough to effectively hinder the adsorption or outgassing, and to withstand to high power and energy lasers, effectively protecting the cladding. In addition, the coating should not decrease the original optical performances of the hollow-core fiber in terms of transmission or light guidance.


In this context, alumina films could be an adequate candidate, as they were already deposited as thin films with good mechanical and optical properties, usually in their crystalline state.^[18] To ensure a good compatibility of use with HC-PCFs, which are submitted to high mechanical constraints and bending, aluminosilicate glasses were favored in this study. In their bulk form, they indeed present a good resistance to high temperatures and good

1. Introduction

In the recent years, the technology of microstructured optical fibers has experienced a tremendous amount of innovation with the introduction of hollow-core photonic crystal fibers (HC-PCF).^[1] Indeed, the internal geometry at the interface of the hollow-core and the microstructuration of the cladding with the well-known Kagome lattice are one of the major key to enhance light confinement and then demonstrate ultralow propagation losses due to the inhibited coupling guidance mechanism.^[2,3] As an example, in the span of 20 years, the losses went

J. Jouin, P. Thomas, H. Orihuel, E. De Sousa, Y. Launay, L. Torzuoli
IRCER: Institut de Recherche sur les Céramiques (UMR CNRS 7315)
Centre Européen de la Céramique
12 rue Atlantis, Limoges Cedex 87068, France
E-mail: jenny.jouin@unilim.fr

H. Orihuel, B. Debord, A. Al-Dhaybi, F. Gérôme, F. Benabid
GPPMM: Gas-Phase Photonic and Microwave Materials
Xlim-UMR CNRS 7572
123 avenue Albert Thomas, Limoges Cedex 87060, France

 The ORCID identification number(s) for the author(s) of this article can be found under <https://doi.org/10.1002/adem.202302209>.

DOI: 10.1002/adem.202302209

hardness while keeping properties from the original silica glass, including its structural organization.^[19] In the form of thin films, this material is chemically inert toward the gas that can be introduced inside the fiber and the coating and can be densified to effectively seal the inner core. It was indeed already used as a chemically inert coating with good anticorrosion properties,^[20] or buffer layer in electronic systems due to its insulating properties or mechanical resistance.^[21] From a compositional point of view, it is close enough to the silica to consider a good adhesion of the coating. Moreover, this material is known as a refractory material with a relatively low thermal conductivity of 14 W mK^{-1} .^[22] Finally, it is also used in optical systems due to their refractive index that can be above 1.6 and high transmission in visible light.^[23] The composition of the films in this system can be modified during the process and plays a role in the optical properties, its refractive index increasing with the Al/Si composition.^[24] As an example, for a composition Al/Si = 2, a refractive index of 1.567 at 633 nm was reported, which is close and slightly above the silica of the original fiber ($n = 1.457$ at 633 nm).^[25]

Most of the aluminosilicate thin films are deposited by physical methods, such as physical vapor deposition,^[26] chemical vapor deposition,^[23,27,28] or radio frequency (RF) magnetron sputtering.^[24] However, some reports are given about thin films deposited by liquid based methods such as spin-coating or dip-coating and presenting very good optical properties.^[29,30] Indeed, in the field of thin films deposition, metal-organic deposition of liquid precursors is a versatile way to obtain low-thickness inorganic thin films.^[31] It can be adapted to different compositions, driven by the required application, and can be suitable to substrates which are not flat, in the case of dip-coating or spray-coating deposition methods.

In this article, we describe the synthesis and deposition of aluminosilicate films on glass substrates of different geometries, the goal being to avoid the gas/surface interaction and increase the lifetime properties of the fibers filled with vapors. The films were deposited from sol-gel chemistry-based solutions, and their chemistry and microstructure was studied. Finally, a coating method was developed to cover the inner core of an HC-PCF and enhance its properties.

2. Experimental Section

The deposit solution, with a metal concentration of 0.8 mol L^{-1} , was synthesized first by the dissolution of aluminum nitrate

nonahydrate (purity > 98%, 7784-27-2, Sigma Aldrich) into absolute ethanol (purity 96%, 64-17-5, Alfa). Then, after complete dissolution, tetraethyl orthosilicate (purity 99.999%, 78-10-4, Sigma Aldrich) was added in the solution with an Al/Si ratio of two and left to mature for 12 h. Three different solutions were prepared. In the first one, the system remained at room temperature for the duration of the synthesis, and in the second one, it was kept at 40°C while in the last one, a reflux of 2 h at 80°C was applied to the mixture. After the syntheses, all the solutions were stored into a fridge.

Differential scanning calorimetry (DSC), thermogravimetry (TG), and X-Ray diffraction (XRD) were used for the powders' characterizations. Thermal analyses were conducted on a simultaneous thermal analyser (STA) 449F3 apparatus from Netzsch using solutions previously dried 24 h at 80°C in air to remove the excess solvent. Approximately 30 mg of powder was deposited in a platinum crucible and then heated up to 1200°C with a heating rate of $10^\circ\text{C min}^{-1}$ in a flow of dry air (100 mL min^{-1}). The powders, previously calcined at 600°C , were also characterized by XRD on a Bruker D8 Advance diffractometer (Bruker, Germany) using $\text{CuK}\alpha$ radiation and equipped with an Anton Paar HTK1200N furnace that could heat the samples up to 1200°C . The room-temperature data were collected over the 2θ angular range of $10^\circ\text{--}70^\circ$ with a step size of 0.016° and an equivalent measured time per step of 174 s, while the in situ data was collected in the same conditions and an exposure time of 149 s per step. The crystalline phases were identified from the experimental patterns using the powder diffraction file (PDF) database of the International Center for Diffraction Data.

The films were deposited by spin-coating onto commercial glass slabs, or by a modified dip-coating method into the HC-PCF. Prior to deposition, the glass substrates were cleaned in hydrogen peroxide to ensure a good wettability by ethanol-based solution.^[32] The glass slabs were coated by spin-coating method (2000 rpm during 30 s). Each layer was dried 10 min at 200°C on a hot plate and the final thermal treatment was performed at 600°C during 1 h in air in a furnace. A Kagome-type HC-PCF was selected for the second study. Its microstructure is represented in **Figure 1**. The left part of the figure shows a general view of the inside of the transverse section of the fiber, the white parts of the image being silica walls, and the black parts being void. These fibers are typical of the geometries that are supposed to be protected. On the right part of the figure, the coating area is represented as a dotted line on the same fiber. The modified dip-coating technique used to coat these areas will be developed further in the publication.

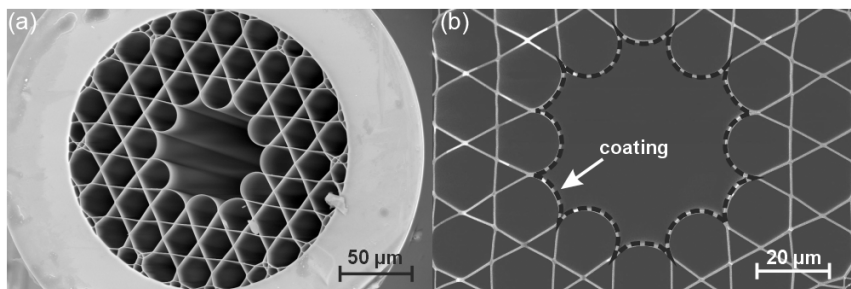


Figure 1. a) SEM image of a Kagome hollow-core fiber; b) identification of the coated surface (dotted line) at the inner core of the sample.

The surface of the coatings deposited on glass slabs was characterized by atomic force microscopy (AFM) to estimate their microstructure and roughness. The measurement was performed using a Bruker Dimension Icon apparatus using contact mode imaging and V-shaped cantilevers for contact mode applications with a typical spring constant of 0.4 N m^{-1} and a nominal radius of the silicon tip of 2 nm (Bruker, Model ScanAsyst-Air). The cross-section images of the fibers were analyzed via scanning electron microscopy (SEM), using a Quanta 450 field emission gun, from field electron and ion company (FEG FEI) microscope. The samples were glued to the sample holder using silver paste and were observed without conductive coating.

The transmission spectra of uncoated and coated fibers were studied by using a homemade supercontinuum source spanning. The white light was then coupled into a fiber piece of approximately 15 cm in length by a set of lenses and mirrors and the detection was made at the fiber output by an optical spectrum analyzer.

3. Results and Discussion

3.1. Characterization of the Coating

The thermal analysis of the xerogel prepared at room temperature is shown in **Figure 2**. Overall the sample lost 57% of its initial mass from room temperature to 600 °C. At 130 °C, a first endothermic peak, associated with a 19.5% mass loss, corresponds to the departure of the water from aluminum nitrate. A second endothermic peak at 241 °C, with a mass loss of 16%, is related to the decomposition of organics from the alkoxide. The remaining mass loss emanates from the decomposition of nitrates and is accompanied by a broad exothermic peak. Finally, a sharp peak with no mass loss can be seen at 989 °C; it is the sign of the crystallization of the aluminosilicate, and it occurs at similar temperature as the crystallization of mullite. The calcination temperature to obtain a fully inorganic and amorphous sample is thus in the temperature range 600–950 °C.

To verify the amorphous nature of the coating, in situ XRD experiment was performed on a xerogel previously calcined 1 h at 600 °C to avoid a volume shrinkage during the experiment. The measured diagrams are presented in **Figure 3**. Note that in this figure the diagram labeled “600 °C” actually corresponds to the sample calcined at 600 °C and then measured at room temperature, while the diagrams from 800 °C were measured in situ. Up to 950 °C, no diffraction peak is visible, thus confirming the existence of a disordered structure. At 1000 °C, well-defined peaks appear and can all be identified with the hypothetical mullite phase $\text{Al}_5\text{SiO}_{9.5}$ (PDF #01-088-2049), although other mullite phases of close compositions can also partially explain the diagram. The formation of this phase is in good agreement with the temperature of the sharp exothermic peak observed in the thermal analysis of **Figure 2**. However, the composition of this crystalline phase does not correspond to the chemical composition of the solution, namely $\text{Al/Si} = 2$, as all phases that could explain the diagram presented a higher aluminum content. This supposes that at such temperatures the crystallization is only partial and that a part of amorphous SiO_2 probably remains in the high-temperature sample.

The solutions, prepared at different temperatures (room temperature, 40 °C or refluxed at 80 °C), were characterized during aging to ensure a good reproducibility of the experiments over time, as it is a requisite for any further technological transfer. For this, thermal analyses were performed on dried solutions after increasingly aging times, from 1 week to 5 months. Between each measurement, the solutions were stored in a fridge in the same conditions as in the coating experiments. Then, the temperatures of the two first endothermic peaks of the crystallization peak and the total mass loss were compared. The broad exothermic peak was not considered, as its position is difficult to define precisely. The results are presented in **Table 1**. First, the final mass loss of the samples is not modified by the process temperature, which is expected as the starting reagents are the same as well as the composition of the solution. The total decomposition of the organics is obtained likewise after a thermal treatment at high temperature. Similarly, the crystallization of the

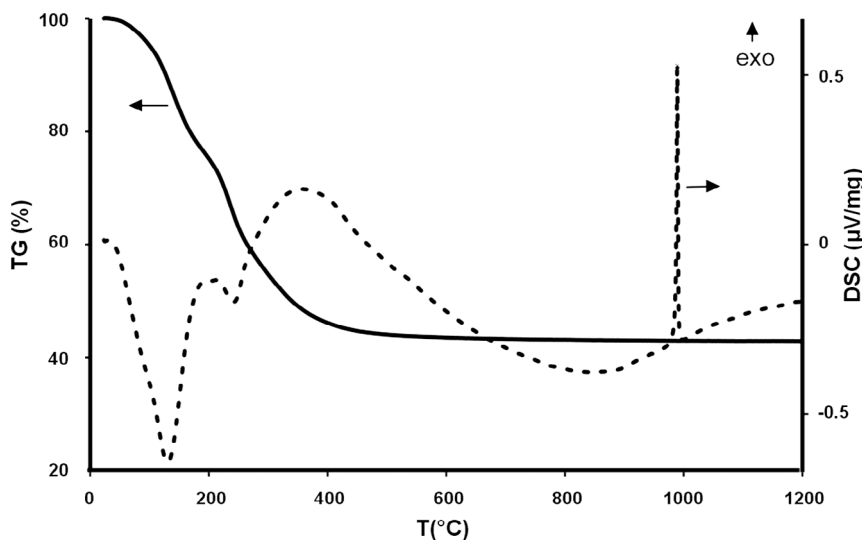


Figure 2. Thermal analysis of an aluminosilicate xerogel previously dried 24 h at 80 °C.

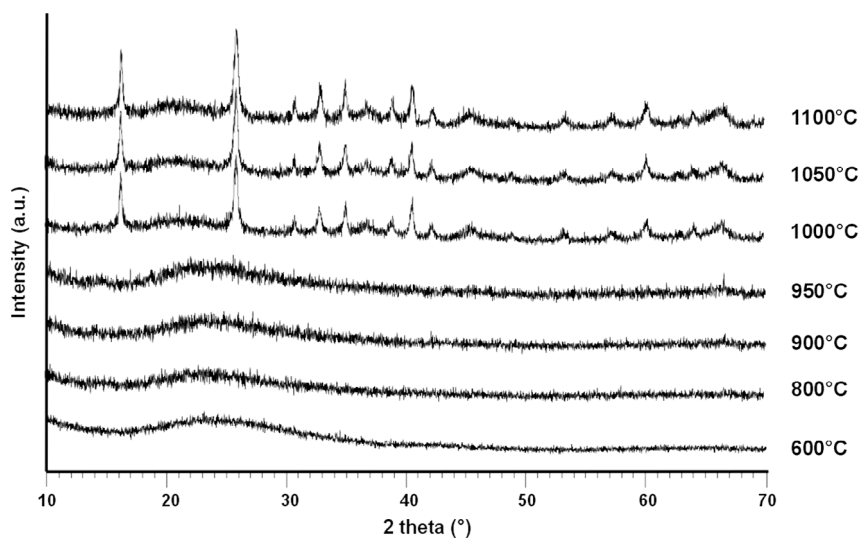


Figure 3. In situ X-ray diffraction diagrams of an aluminosilicate sample pre-calcined at 600 °C.

Table 1. Standard deviations observed on the values of thermal events and mass loss measured by TG/DSC of solutions synthesized at different temperatures.

| Synthesis temperature | Aging time | Standard deviation from the average value | | | |
|-----------------------|------------|---|------------------|------------------|------------------|
| | | Peak 1 130 °C | Peak 2 240 °C | Peak 3 990 °C | Mass loss 57% |
| 20 °C | 1 month | 3 | 2 | 1 | 1 |
| | 2 months | 12 | 10 | 1 | 1 |
| | 3 months | 3 | 3 | 1 | 2 |
| | 4–5 months | 2 | 9 | 1 | 2 |
| 40 °C | 1 month | 6 | 3 | 1 | 1 |
| | 2 months | 4 | 5 | 1 | 1 |
| | 3 months | 3 | 5 | 0 | 1 |
| | 4–5 months | 15 | 3 | 0 | 2 |
| 80 °C | 1 month | 5 | 5 | 1 | 1 |
| | 2 months | 10 | 6 | 1 | 2 |
| | 3 months | 12 | 8 | 1 | 2 |
| | 4–5 months | 4 | 11 | 0 | 3 |

mullite phase occurs at the same temperature, regardless of the synthesis history. However, the thermal events occurring at lower temperature, namely the peaks 1 and 2, are more sensitive to the synthesis conditions. In particular, for the solution prepared at room temperature, a perturbation occurs during the second month, with a stabilization for longer storage times. This could be the sign of a noninitially stabilized solution due to a too little amount of energy given to the system, the finalization of the condensation occurring at a later stage. In the case of a synthesis at 40 °C, the values are quite stable for the 3 first months, and after this period, the first peak starts to show dispersed values. This could give a utilization duration of 3 months for this solution. In the case of a solution prepared with a reflux at

80 °C, the initial values are stable, but the solution becomes unstable more quickly. Finally, for the following experiments, the solution prepared at 40 °C was selected, as it was the most reliable for the duration of the experiments.

Prior to the deposition process, the glass slabs used for the spin-coating were chemically cleaned in H₂O₂ for 30 min at room temperature to enhance their wettability by the ethanol-based solutions. Their contact angle indeed decreased from 22° for the as-received surfaces to a complete spreading of the droplet after the cleaning procedure. **Figure 4** shows the surface of the substrates before and after the chemical bath. In both cases, the surface is rougher than what was expected for glass, with surface roughness Sa of 0.26 and 0.43 nm, respectively. The topography is also similar for the two substrates, showing a large very flat background and small dots distributed on the whole area. It seems that the cleaning modifies the chemical properties of the surface with no physical modification or degradation.

These cleaned substrates were selected for spin-coating deposition using solutions with metal concentration of 0.8 or 0.1 mol L⁻¹. The microstructures of the coatings obtained with one or multiple iterations are represented in **Figure 5**. The films deposited with high concentrated solution display a smooth and homogeneous microstructure for the first layer (**Figure 5a**) with Sa = 0.16 nm. A small number of fissures was noticed at various places of the film, without being directly correlated to a border effect occurring during the spin-coating. When increasing the number of depositions, the film presented a high number of cracks, which formed during the evaporation of the solvent. This phenomenon is common for films deposited with a high thickness per layer related with highly concentrated solutions. For this reason, the depositions were stopped after two layers. The microstructure of the film, away from the cracks, is characterized by the same configuration as the first layer, with Sa = 0.16 nm and the presence of a fine grain topography (**Figure 5b**). However, this concentration is not suitable for this kind of deposition on a large scale as it cannot be obtained without macrostructural defects. In the case of a diluted solution

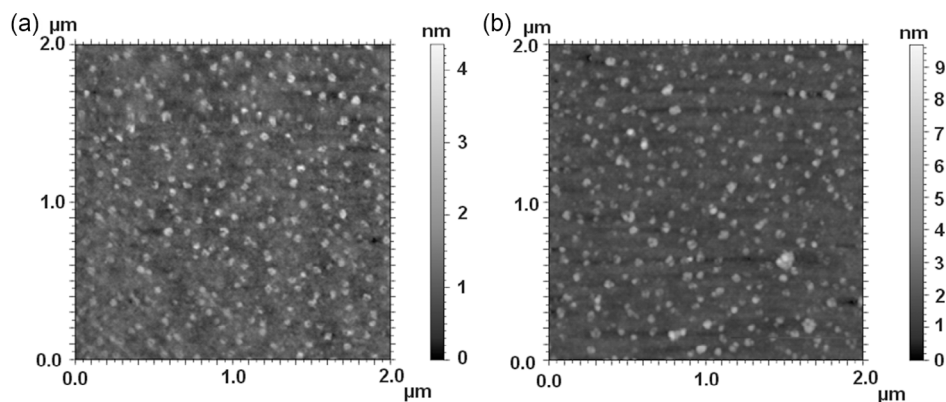


Figure 4. AFM surface image of the glass substrates: a) as received and b) after a chemical cleaning in hydrogen peroxide.

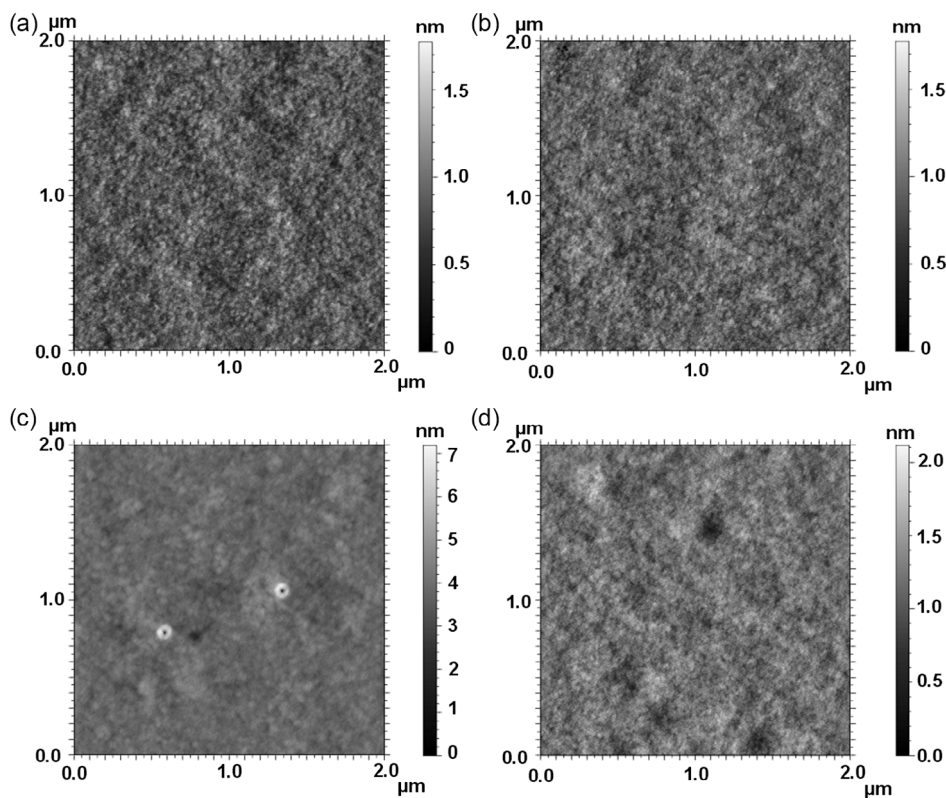


Figure 5. AFM images of the surface of coatings prepared with different concentrations and number of layers: a) $C = 0.8 \text{ mol L}^{-1}$, 1 layer; b) $C = 0.8 \text{ mol L}^{-1}$, 2 layers; c) $C = 0.1 \text{ mol L}^{-1}$, 1 layer; and d) $C = 0.1 \text{ mol L}^{-1}$, 5 layers.

($C = 0.1 \text{ mol L}^{-1}$), the first layer's topography (Figure 5c) is irregular and some porosity is visible in the coating, originating from bubbles. Its roughness is $S_a = 0.25 \text{ nm}$, which is still lower than the one of the substrate alone, showing its covering properties even in the first stages on the process. The deposition of five layers was possible with this solution, and no cracking of the transparent coating occurred. The microstructure of its surface, shown in Figure 5d, is closer to what was observed for the undamaged parts of films deposited from the 0.8 mol L^{-1}

solution, with $S_a = 0.17 \text{ nm}$. Overall, the observed microstructures are similar to the ones observed after a dip-coating deposition for the same Al/Si composition and doping with Er^{3+} .^[33] Moreover, the measured roughness using this deposition method is lower than what was measured on similar composition film deposited via RF magnetron sputtering (about 2 nm).^[24] In conclusion, it appears that it is possible to obtain a smooth, inorganic, and amorphous aluminosilicate film on a glass substrate by using this solution as a precursor.

3.2. Development of a Coating inside a Hollow-Core Fiber

The previously characterized solutions were used to develop an original coating method of the internal wall of an HC-PCF. First, due to their diluted nature, the rheological properties of the solutions were similar to the ones of ethanol, meaning that the viscosity was very low, regardless of their metal concentration. This is a requirement to ensure the flow of liquid in the small diameter core (a few tens of microns) of the fiber. Then, the fiber was prepared to ensure that the coating solution would be in contact with the inner core and not the rest of the cladding. For this purpose, the ending of the fiber was partially collapsed with a controlled heating to melt the capillary network that surrounds the central core. A picture of an as-prepared fiber, taken during the process, is shown in **Figure 6**. The melted ending of the fiber was then plunged into the coating solution, which was pumped inside using a primary vacuum pump until the solution reached the other end. Note that the pumping should be stopped immediately after the liquid is visible, and not be repeated after the first run, to avoid the ceramic coating to start clogging the inner core as shown in **Figure 7a,b**. The typical length of the fiber at this stage is 1 m. This ensures a coating procedure which is short

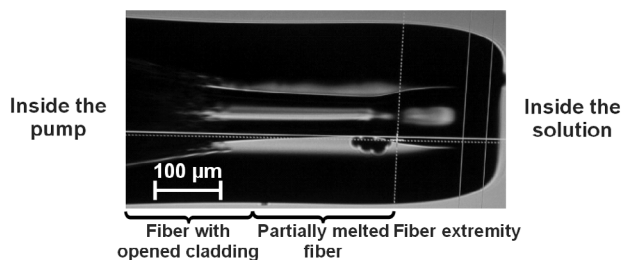


Figure 6. Picture of the melted end of a prepared fiber.

enough to avoid this clogging to occur. During the coating process, the solution is first deposited successfully at the inner core of the fiber with no contact with the cladding network (**Figure 7c**). Then, a first shrinkage occurs during the drying of the solvent, which occurs at 80 °C during 24 h in an oven (**Figure 7d**). However, at this stage, the deposited layer still contains an abundant organic part, as seen in the thermal analysis. The ceramic coating is fully inorganic after a thermal treatment at 600 °C in a furnace, and the subsequent shrinkage that occurs during the pyrolysis step is visible in **Figure 7e**, where the coating is hardly visible. This step was performed on 20–40 cm samples, as the size of the isothermal zone of the tubular furnace could not exceed this value. This was still coherent with the targeted applications (metrology, gas detection), as they require less than 20 cm fibers for their use. The further development of this coating procedure for longer samples might require either an adaptation of the heating device, probably associated with a modification of the coating solution. The final thermal treatment of the fibers, unlike the one of the flat films, was performed at a low heating rate (1 °C min⁻¹) instead of 10 °C min⁻¹ used in most cases to avoid a too brutal release of the organics in such a confined environment. This heating rate indeed leaves a sufficient time for the organics to be properly evacuated for samples up to 40 cm in length but can be adapted for different length/core diameter ratios.

After the calcination, the films are dense, relatively thin which leave a large volume to encapsulate gas inside the core, and homogeneous (**Figure 7e**). However, as for the samples deposited on plane substrates, the concentration of the precursor solution has a direct influence on the thickness of the coating and thus its quality. Due to the complex shape of the substrate, it was not necessary to work with concentrated solutions, which would lead to excessively thick coatings. In **Figure 8**, films prepared using coating solutions with concentrations of 0.8 and

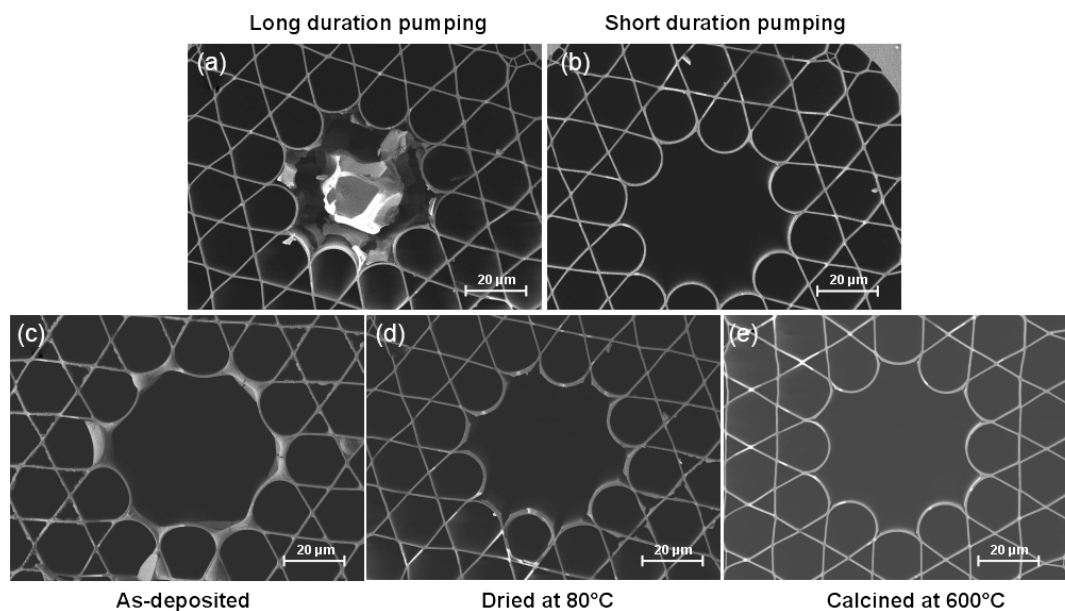


Figure 7. SEM pictures of the fibers during the coating. a) Clogged fiber due to an extended duration process and b) properly coated fiber. c) Solution deposited in the core of the fiber: d) after the drying of the solvent and e) after a calcination at 600 °C (final fiber).

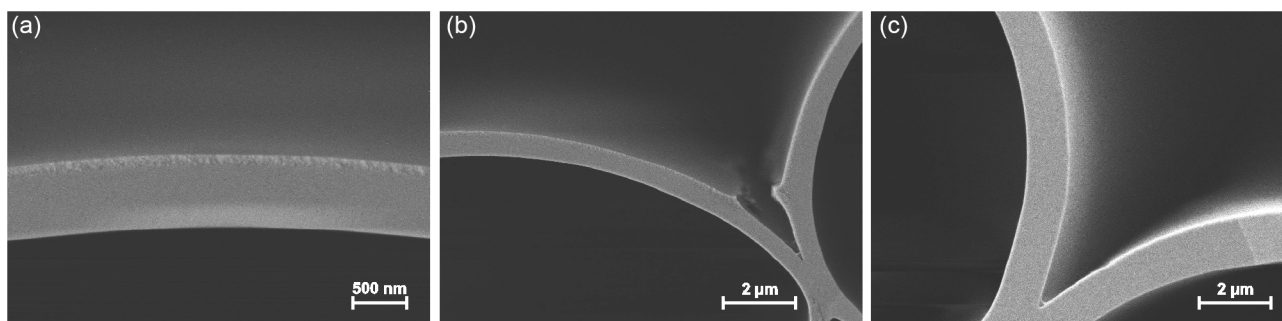


Figure 8. Aluminosilicate films calcined at 600 °C. a,b) Solution concentration of 0.8 mol L⁻¹ and c) solution concentration of 0.1 mol L⁻¹.

0.1 mol L⁻¹ were deposited, dried at 80 °C and calcined at 600 °C in the same way. During the process, a few cross-section images of the samples were taken from different parts of the fiber and show very similar thicknesses. The images presented in the following represent what was observed all along the samples. Figure 8a,b shows the microstructure of the film obtained with the high concentration. On the convex part of the core, the coating appears dense and without any defect, with a thickness of approximately 100 nm. However, upon observation of the acute angles, which are characteristics of the geometry of the core, aggregation of material leads to the systematical formation of cracks during the degradation of organics. Decreasing the solution concentration to 0.4 mol L⁻¹ did not improve this point, as occasional cracks could still be observed. Finally, the film deposited using a 0.1 M solution, Figure 8c, is much thinner, with a thickness of 20–30 nm. There are no cracks in the acute angles, as only a small aggregation is visible on the SEM image. Note that these concentrations are subjected to vary slightly in the case of a geometry modification on the fiber, which occurs when changing the application. In all cases, the coating inside the core seems to be smooth, the development of an optical profilometer is currently under investigation for an accurate characterization of these samples.^[11] It should give access to the probable increase of the surface roughness to estimate its potential influence on the

losses of the fibers. The fibers with the continuous aluminosilicate coatings were then selected for characterization.

First, the transmission of coated fiber was compared to the original one, the result being shown in **Figure 9**. Note that in this measurement, due to the limited length of the samples, the injection conditions were not strictly identical for all the samples, which could lead to differences in the power level that are not related with the presence of the coating. In this case, only the spectral position of the bands can be analyzed. The transmission window is found similar for both samples, and the transmitted single mode is preserved. The ceramic coating can thus be applied without modifying the original optical and guiding properties of the HC-PCF, keeping it optimized for the application as an atomic vapor cell. Moreover, the increased lifetime of rubidium inside the core was assessed by our team,^[13,15] and it was shown that the gas was not adsorbed and still detectable more than 1 month after the filling of the fiber, instead of a few hours, which establish the good sealing of the inner surface. On the same subject, the outgassing of the fibers' chemicals inside the core, which tended to decrease its properties overtime, was also inhibited for at least 1 year.^[16] The use of this coating for its antirelaxation properties was considered and its results were compared with other non-ceramic coatings deposited by the same way, their performances were slightly better than an

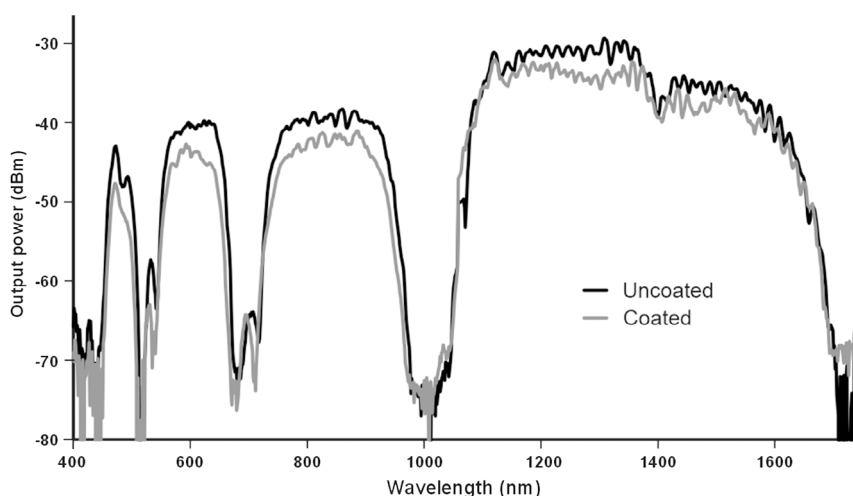


Figure 9. Transmission of light from a raw fiber and an aluminosilicate-coated one.

uncoated fiber.^[34,35] Finally, the fibers withstand the transportation of light without damaging the coating. The coated samples, used in contact with gas (Rb^[13,15] or iodine^[36]), showed a good stability of their properties overtime.

4. Conclusion

Aluminosilicate protective coatings of the inner walls of HC-PCFs have been optimized by using an original deposit method. That one was based on coating of the inside of the fiber core by pumping a sol-gel solution. The Al/Si = 2 solution was developed on flat substrates and gave smooth, amorphous, and inorganic layers after annealing at 600 °C. Inside the fibers, the use of a diluted solution (C = 0.1 mol L⁻¹) gave thin (20–30 nm), dense, inorganic, and amorphous layers transmitting in selected wavelengths from the UV to IR range after the optimization of the processing parameters.

It was demonstrated that these aluminosilicate ceramic coatings allow increasing the lifetime of the original fibers filled when used with rubidium vapor. Moreover, an interesting result is that the original guiding properties of the uncoated fiber are conserved. These promising results and especially the adapted method of coating inside the inner core of a fiber by pumping a chemical solution could open a large field of research in the area of new optical properties and applications of gas/vapor-filled HC-PCFs. In particular, the investigation of new compositions of ceramic coatings or multimaterials could be one of these challenges.

Acknowledgements

This work was supported by institutional grant from the National Research Agency under the Investments for the future program with the reference ANR-10-LABX-0074-01 Sigma-LIM and Région Nouvelle Aquitaine under OzoneFinder and AAPR2020A-2019-8206410 projects. The authors also wish to thank Valérie Coudert, Sylvie Rossignol, and Lila Ouamara for their help concerning atomic force microscopy, rheology, and surface wettability assessments.

Conflict of Interest

The authors declare no conflict of interest.

Data Availability Statement

The data that support the findings of this study are available from the corresponding author upon reasonable request.

Keywords

aluminosilicates, atomic force microscopies (AFMs), chemical solution depositions, coatings, hollow-core photonic crystal fibers (HC-PCFs), microstructures, scanning electron microscopies (SEMs)

Received: December 21, 2023

Revised: February 20, 2024

Published online:

- [1] R. F. Cregan, B. J. Mangan, J. C. Knight, T. A. Birks, P. S. J. Russell, P. J. Roberts, D. C. Allan, *Science* **1999**, *285*, 1537.
- [2] F. Benabid, J. C. Knight, G. Antonopoulos, P. S. J. Russell, *Science* **2002**, *298*, 399.
- [3] F. Couny, F. Benabid, P. J. Roberts, P. S. Light, M. G. Raymer, *Science* **2007**, *318*, 1118.
- [4] G. T. Jasion, H. Sakr, J. R. Hayes, S. R. Sandoghchi, L. Hooper, E. N. Fokoua, A. Saljoghei, H. C. Mulvad, M. Alonso, A. Taranta, T. D. Bradley, I. A. Davidson, Y. Chen, D. J. Richardson, F. Poletti, *Optics InfoBase Conf. Papers*, Th4C.7, Optica Publishing Group, OSA, Washington **2022**.
- [5] T. A. Birks, J. C. Knight, P. St. J. Russell, *Opt. Lett.* **1997**, *22*, 961.
- [6] F. Benabid, P. J. Roberts, *J. Mod. Opt.* **2011**, *58*, 87.
- [7] B. Debord, F. Amrani, L. Vincetti, F. Gérôme, F. Benabid, *Fibers* **2019**, *7*, 16.
- [8] Y. Y. Wang, N. V. Wheeler, F. Couny, P. J. Roberts, F. Benabid, *Opt. Lett.* **2011**, *36*, 669671.
- [9] B. Debord, M. Alharbi, T. Bradley, C. Fourcade-Dutin, Y. Y. Wang, L. Vincetti, F. Gérôme, F. Benabid, *Opt. Express* **2013**, *21*, 28597.
- [10] M. Alharbi, T. Bradley, B. Debord, C. Fourcade-Dutin, D. Ghosh, L. Vincetti, F. Gérôme, F. Benabid, *Opt. Express* **2013**, *21*, 28609.
- [11] J. H. Osório, F. Amrani, F. Delahaye, A. Dhaybi, K. Vasko, F. Melli, F. Giovanardi, D. Vandembroucq, G. Tessier, L. Vincetti, B. Debord, F. Gérôme, F. Benabid, *Nat. Commun.* **2023**, *14*, 1146.
- [12] T. D. Bradley, Y. Wang, M. Alharbi, B. Debord, C. Fourcade-Dutin, B. Beaudou, F. Gérôme, F. Benabid, *J. Light. Technol.* **2013**, *31*, 2752.
- [13] T. D. Bradley, E. Ilinova, J. J. McFerran, J. Jouin, B. Debord, M. Alharbi, P. Thomas, F. Gerome, F. Benabid, *J. Phys. B: At., Mol. Opt. Phys.* **2016**, *49*, 185401.
- [14] B. Debord, F. Amrani, L. Vincetti, F. Gérôme, F. Benabid, *Fibers* **2019**, *7*, 58.
- [15] T. D. Bradley, J. Jouin, J. J. McFerran, P. Thomas, F. Gerome, F. Benabid, *J. Light. Technol.* **2014**, *32*, 2486.
- [16] M. Chafer, Thesis, Limoges University, **2018**.
- [17] B. Debord, F. Gérôme, P. Paul, A. Husakou, F. Benabid, *2015 Conf. Lasers and Electro-Optics Proc.*, STh4L.7, Optica Publishing Group, OSA, Washington **2015**.
- [18] P. Nayar, A. Khanna, D. Kabiraj, S. R. Abhilash, B. D. Beake, Y. Losset, B. Chen, *Thin Solid Films* **2014**, *568*, 19.
- [19] L. Cormier, in *Encyclopedia of Materials: Technical Ceramics and Glasses*, Elsevier, Oxford **2021**.
- [20] V. A. C. Haanappel, H. D. van Corbach, T. Fransen, P. J. Gellings, *Surf. Coat. Technol.* **1994**, *63*, 145.
- [21] N. Komatsu, K. Masumoto, H. Aoki, C. Kimura, T. Sugino, *Appl. Surf. Sci.* **2010**, *256*, 1803.
- [22] Y. Zhao, Z. Zhai, D. Drummer, *Polymers* **2018**, *10*, 457.
- [23] D. H. Kuo, B. Y. Cheung, R. J. Wu, *J. Non-Cryst. Solids* **2003**, *324*, 159.
- [24] R. Magnusson, B. Paul, P. Eklund, G. Greczynski, J. Birch, B. Jonson, S. Ali, *Vacuum* **2021**, *187*, 110074.
- [25] I. H. Malitson, *J. Opt. Soc. Am.* **1965**, *55*, 1205.
- [26] V. A. C. Haanappel, H. D. van Corbach, T. Fransen, P. J. Gellings, *Surf. Coat. Technol.* **1994**, *63*, 145.
- [27] A. W. Apblett, L. K. Cheatham, A. R. Barron, *J. Mater. Chem.* **1991**, *1*, 143.
- [28] A. Teiserskis, A. Zukova, Y. K. Gun'ko, S. Grudinkin, T. S. Perova, R. A. Moore, *Thin Solid Films* **2006**, *515*, 1830.
- [29] Y. Y. Chen, W. C. J. Wei, *J. Eur. Ceram. Soc.* **2001**, *21*, 2535.
- [30] E. Gutmann, A. A. Levin, I. Pommrich, D. C. Meyer, *Cryst. Res. Technol.* **2005**, *40*, 114.
- [31] R. W. Schwartz, T. Schneller, R. Waser, *C. R. Chim.* **2004**, *7*, 433.
- [32] J. J. Cras, C. A. Rowe-Taitt, D. A. Nivens, F. S. Ligler, *Biosens. Bioelectron.* **1999**, *14*, 683.

- [33] M. Benatsou, B. Capoen, M. Bouzaoui, W. Tchana, J. P. Vilcot, *J. Sol-Gel Sci. Technol.* **1998**, *13*, 529.
- [34] X. M. Zheng, J. Jouin, M. Delgrange, C. Restoin, B. Debord, P. Thomas, F. Jérôme, F. Benabid, in *2018 Conf. on Lasers and Electro-Optics Proc.*, 8427697, Optica Publishing Group, OSA, Washington **2018**.
- [35] X. M. Zheng, M. Delgrange, J. Jouin, P. Thomas, B. Debord, F. Jérôme, F. Benabid, *2018 Conf. on Lasers and Electro-Optics Proc.*, 8427696, Optica Publishing Group, OSA, Washington **2018**.
- [36] C. Goïcochéa, T. Billotte, M. Chafer, M. Maurel, J. Jouin, P. Thomas, D. Naik, F. Jérôme, B. Debord, F. Benabid, *Opt. Express* **2023**, *31*, 15316.